Analytical Methods

Accepted Manuscript

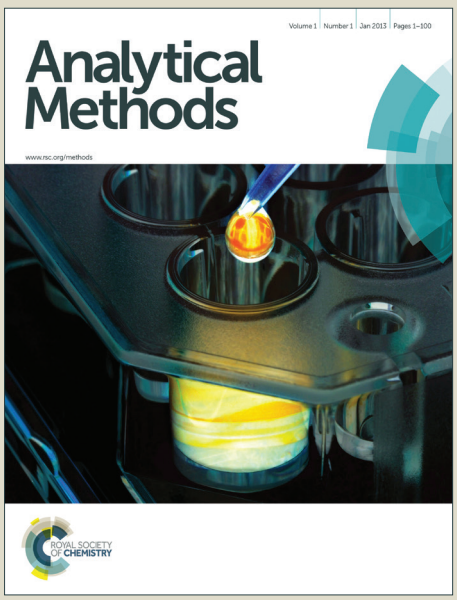

ROYAL SOCIETY OF CHEMISTRY

www.rsc.org/methods

^{13}C stable isotope labeling followed by ultra-high performance liquid chromatography/quadrupole time-of-flight tandem mass spectrometry (UHPLC/Q-TOF MS) was applied to identify the metabolites of honokiol in rat small intestine

Na Ye[a, b, #], Minghai Tang[b, #], Haoyu Ye[b], Chunyan Wang[a], Chunyu Wang[b], Qiunan Yang[a], Li Wan[a]*, Lijuan Chen[b]*

[a]: School of Pharmacy, Chengdu University of TCM, The Ministry of Education Key Laboratory of Standardization of Chinese Herbal Medicine, State Key Laboratory Breeding Base of Systematic Research, Development and Utilization of Chinese Medicine Resources, Chengdu 611137, China

[b]:State Key Laboratory of Biotherapy, West China Hospital, West China Medical School, Sichuan University, Keyuan Road 4, Gaopeng Street, Chengdu 610041, China

***Correspondence author:**

Prof. Li Wan

School of Pharmacy, Chengdu University of TCM, The Ministry of Education Key Laboratory of Standardization of Chinese Herbal Medicine, State Key Laboratory Breeding Base of Systematic Research, Development and Utilization of Chinese Medicine Resources, Chengdu, China

E-mail: wanli8801@163.com

Prof. Lijuan Chen

State Key Laboratory of Biotherapy, West China Hospital, West China Medical School, Sichuan University, Keyuan Road 4, Gaopeng Street, Chengdu 610041, China

E-mail: lijuan17@hotmail.com

[#] these two authors contributed equally to this paper.

Abstract

Honokiol, as a pharmacologic active small-molecule, received significant attention for its strong pharmacological effects without remarkable toxicity. However, the metabolites of honokiol in small intestine, one of the most important extrahepatic site of drug biotransformation are unknown. In this article, a method of ^{13}C stable isotope labeling followed by ultra-high performance liquid chromatography/quadrupole time-of-flighttandem mass spectrometry (UHPLC/Q-TOF-MS) was applied to identify the metabolites of honokiol in rat small intestine. According to the unique isotopic patterns that two peaks with similar intensities ratio nearly 1:1 and molecular weight difference of 6 Da between honokiol and ^{13}C-labeled honokiol, a total of 20 metabolites were observed and tentatively characterized in small intestine, eight of which were reported firstly. All of them were phase II metabolites and divided into sulfate, amino acids conjugated and glucuronide metabolites. This study combined with previously paper reported about honokiol metabolites in rat feces, plasma and urine will benefit for further studying the metabolism and action mechanism of honokiol in vivo.

Key Word: Honokiol; Metabolite; Small intestine; UHPLC/Q-TOF-MS; ^{13}C-label

1. Introduction

Honokiol (as shown in Fig.1) is a biphenolic constituent isolated and purified from the stem bark and root of *Magnolia officinalis* which has been used to treat various diseases in Asian for thousands of years, especially in China, Japan, and Korea [1]. It has been shown to possess wide pharmacological action and clinical application, including anti-anxiety, anti inflammatory, anti-alcoholic fatty liver, anti-oxidative [2-10]. In a recent study, honokiol showed remarkable anti-tumor effects on various cancer cell lines [11-13]. Up to date, investigation about honokiol is a growing subject of research for its multifarious and strong pharmacological effects without remarkable toxicity [7], and the metabolism of honokiol in tissues have not been paid much attention. Therefore, our aim here was to identify the honokiol metabolites in rat small intestine to probe into the metabolites of honokiol further.

Small intestine plays a significant role in absorption and metabolism of beneficial nutrient and potentially harmful xenobiotic [14-15]. It not only has many transporters, but also expresses a range of both phase I and phase II metabolic enzymes [14,16-21]. Mequindox, glucuronidase and testosterone could be metabolited in small intestine though different enzymes [22-24]. Besides, large numbers of bacteria and their respective enzymes in small intestine also have the ability to metabolize drugs or drug conjugates. Digoxin could be metabolized to DRP by microbiota [25]. Ginsenosides Rg3 formed Rh2 and PPD which have stronger antitumor activity via intestine microbiota [26]. In view of the particularity of small intestine metabolism, and the metabolites of honokiol in tissues are not been known, investigation of metabolites in small intestine can make clear of the overall metabolism and the clinical applications of a potential drug candidate.

Ultra-high performance chromatography/quadrupole time-of-flight tandem mass spectrometry (UHPLC/Q-TOF-MS) coupled with stable isotope labeling as a fantastic and increasingly popular technique have been widely used in the fields of drug analysis, pharmacokinetics and other biologic samples for its better resolution, accurateness and sensitivity [27-30]. Previously, we have successfully used this method

to separate and tentatively identify 18, 57 and 42 honokiol metabolites in rat plasma, urine and feces, respectively [31-33]. By this approach, twenty metabolites were observed and tentatively identified in rat small intestine, eight of which were first time to be reported and their possible fragmentations have also been deduced.

2. Experimental

2.1 Chemicals and reagents

Honokiol (purity ≥98%) was separated and purified in our laboratory as previously described [34]. Honokiol-[$^{13}C_6$]-labeled (purity >98%) was purchased from the Wuxi Beita Company (Wuxi, Jiangsu China). HPLC-grade Methanol and Ethylacetate were obtained from Fisher Scientific (Fairlawn, NJ, USA). Ultrapure water was produced by the Milli-Q Ultrapure water purification system (18.5MΩ) (Millipore Corp., Bedford, MA, USA). All the other chemicals and solvents used in this experiment were of analytical grade.

2.2 Animals and animal experiments

Male Sprague-Dawley rats (120-180g, 6-7weeks old) were obtained from Beijing HFK Bioscience Co., Ltd. (Beijing, China), and were kept under the constant condition: temperature (22–24°C), humidity (55–65%), and lightening (12 h light per day). The rats were fasted overnight while free access only to water before the experiment. All the Animal experimental procedures were complied with the guidelines of the Animal Ethics Committee of Sichuan University. Honokiol and Honokiol-[$^{13}C_6$]-labeled were injected with the amount of 40 mg/kg of body weight via tail vein.

2.3. Sample preparation

Rats were anaesthetized by intraperitoneal injection of 10% chloral hydrate (0.3 ml per 100g body weight). Small intestine was removed and immediately washed with 0.9% NaCl solution, stored at-20°C until analysis. Blank small intestine samples were obtained from the untreated rats.

The samples were crushed by liquid nitrogen, and then an aliquot of intestine sample (200mg) were transferred to a clean test tube (1.5 mL) and mixed with ethyl acetate (1 mL). The mixture was vortexed for 3min then centrifuged at 13,000 rpm for 10 min, all the supernatant was transferred to another clean test tube. The lower precipitation maxed with methanol (1 mL) to make the extracting sufficient, the followed procedures about vortex and centrifugation were same as above mentioned. Merging the two supernatant, and then evaporated to dryness under nitrogen at 45°C. The residue was reconstituted in 200 μL of mobile phase (methanol/water=25/75), then centrifuged at 13,000 rpm for 15 min, last injected into the UPLC/Q-TOF-MS system for analysis (5 μL injection volume). Besides, the blank sample was processed at the same way.

2.4. Apparatus and chromatographic conditions

Chromatographic analyses were performed on UHPLC™ BEH C_{18} column (50 mm×2.1 mm I.D., 1.7 μm, waters) with the column temperature was set at 30°C, the temperature of sample was maintained at 10°C. The total run time was 30 min, which at a flow rate of 0.25 mL/min with a linear gradient running form 25% to 75% B (methanol). The injection volume was 5 μL per sample.

ESI-Q-TOF-MS/MS ananalysis were achieved on Waters ACQUITY UHPLC™ system (Waters Corp., Milford, MA, USA) coupled to a Waters Q-TOF Premier mass spectrometer (Waters Corp., Milford, MA, USA) through an ESI interface operating in negative mode. The ESI source parameters were as follows: capillary voltage 2.8 kV, cone voltage 20 kV, source temperature 90°C, desolvation temperature 200°C, and desolvation gas (N_2) with a flow rate of 300L/h. As for the Q-TOF-MS/MS experiment, flow rate of the collision gas (Ar) was 0.45 L/h, collision energy was 20–35 eV. The MS and MS/MS acquisition rate was set to 1.0 s with a 0.02s inter-scan delay. Data were acquired from 100 Da to700 Da. The instrument was controlled, all the data were acquired and processed by Masslynx™ 4.1 software (Waters Corp., Milford, MA, USA).

3 Results and discussion

3.1 Discovery of metabolites

As previously reported [31-33], an equimolar mixture of honokiol and ^{13}C-labeled honokiol was administered to the rats by caudal vein leading to two peaks in MS spectra. So through the full scan mass spectra of experimental sample in comparison with blank sample (Fig 2), we could find the potential metabolites according to similar intensities ratio of two peaks and the mass shift of 6 Da (one benzene ring of honokiol was labeled by ^{13}C), as presented in Fig. 3. By analyzing the fragment ions, cleavage behavior and comparing with previous reports, we discovered and characterized honokiol metabolites in small intestine comprehensively.

The data of detected metabolites including retention times, MS/MS fragments, and molecular formulas were summarized in Table 1. Meanwhile, metabolites structures were shown in Fig. 4, four metabolites as the representative of MS/MS fragmentation were exhibited in Fig. 5.

3.2 Identification and structure elucidation of metabolites

The parent drug was detected at a retention time of 23.136min, giving a adduct ion of chloride at *m/z* 301.1002 $[M+Cl]^-$. No phase I metabolites were detected, instead 20 phase II metabolites of honokiol were observed and divided into 4 sulfate conjugates, 12 amino acids conjugates and 4 glucuronide metabolites.

3.2.1 Mono-sulfate conjugates (M2, M5, M9, M10)

Sulfate conjugation is one conventional type of conjugation reaction with the neutral loss of 80Da [35]. M2 (t_R = 1.813 min) gave a deprotonated molecular ion $[M–H]^-$ at *m/z* 349.0389. Abundant specific fragment ions were identified at *m/z* 269, 225, 209, 184, 183. The neutral loss of SO_3 (80 Da) formed the prominent fragment ion at *m/z* 269 $[M-H-80]^-$ suggesting M2 was sulfate conjugation metabolite. The one at *m/z* 269 was dissociated into *m/z* 225$[M–H-80-44]^-$, ascribed to the elimination of CO_2. As for ion at *m/z* 209 resulted from the one at *m/z* 225 was due to the *ortho*-allyl generated a five-membered ring, it led to the fragment ion at *m/z* 183 by its further cleavage. But we could not define the exact position of sulfate conjugation for honokiol possessed two phenolic hydroxyl groups. Therefore, M2 was formed though

oxidized *para*-allyl of honokiol into carboxyl, and then one phenolic hydroxyl group conjugated with sulfate.

M5 (t_R = 2.497 min) yielded a deprotonated ion $[M–H]^-$ at *m/z* 375.0541. In the MS/MS spectrum, it showed the fragment ions at *m/z* 295, 251 and 210, which were the same as J.Liu et al [31]. A predominant ion at *m/z* 295 $[M-H-80]^-$ indicated M3 was a sulfate conjugation metabolite, which further lost a neutral moiety of CO_2 to form ion at *m/z* 251 $[M-H-80-44]^-$. According to these fragment ions, the accurate site of sulfate conjugation couldn't be fully ascertained likewise.

M9 (t_R = 7.592 min) was observed $[M–H]^-$ at *m/z* 361.0735 in UHPLC/Q-TOF-MS spectrum. The MS^2 spectrum gave fragment ions at *m/z* 281, 240 (see Fig. 5(a)). The one at *m/z* 281 $[M–H-80]^-$ indicated the loss of SO_3 (80Da), implying M2 was a sulfate conjugation product. The *ortho*-allyl group may be oxidized to hydroxyl with the position of C=C double bond changed[36], then generated a five-membered ring by losing two hydrogen atoms, the free radical product ion at *m/z* 240 was yield due to the cleavage of *para* -allyl radical.

The full scan mass spectrum of M10 (t_R = 8.789 min) exhibited a deprotonated ion $[M-H]^-$ at *m/z* 403.0851. The presence of the dominating fragment ion at *m/z* 263 $[M-H-80-42-18]^-$ was identical to the consecutive losses of SO_3 (80Da), C_2H_2O (42Da) and H_2O (18Da). Therefore, M10 was proposed as sulfated and acetylated metabolite. In view of phenolic sulfates the loss of SO_3 (80 Da), while aliphatic sulfates loss of HSO_4 (97 Da) in negative ionization mode [37], the sulfate conjugation occurred at C-2 position.

As what has been discussed above, M2, M5, M9 and M10 were endowed with the characteristic of neutral loss of SO_3 (80 Da), which provided the most sufficient evidence of they were sulfate conjugation metabolites. In addition, the probably structures of them were consistent with previous inference [31-33]. It was a pity that owing to the lack of reference standard and honokiol contained two phenolic hydroxyl groups at C-2 and C-4' position, respectively. We could not define the veracious position of sulfate conjugation. The possible structures of M2, M5, M9 and M10 were shown in Fig. 4.

3.2.2 Amino acids conjugated metabolites (M1, M3, M6-M8, M14-M20)

Generally, amino acids conjugated metabolites always occur in the nature of distinctive mass shift such as 57 (C_2H_3NO) for glycine conjugates, 87 ($C_3H_5NO_2$) for serine conjugates, 129 ($C_5H_7NO_3$) for glutamic acid conjugates, 114 ($C_4H_6N_2O_2$) for asparagine conjugates. The possible structures of amino acids conjugated metabolites were also shown in Fig. 4.

M1 (t_R = 1.522 min) exhibited a deprotonated ion $[M-H]^-$ at *m/z* 482.1926 and produced a collection of fragment ions at *m/z* 281, 263, 224. The fragment ion at *m/z* 281 $[M-H-C_3H_6NO_2-C_4H_7N_2O_2-]^-$ implied that M1 was serine and asparagine conjugation product. The main one at *m/z* 281 undergoing afterwards departure of a molecule of water brought out the fragment ion at *m/z* 263 which caused the one at *m/z* 224 via cleavage of allyl radical at C-5 position. Thus, M1 maybe generated by that *para*-allyl underwent hydroxylation, while the *ortho*-allyl formed a six-membered ring, and then phenolic hydroxyl at C-2 position and *para* aliphatic hydroxyl conjugated with serine and asparagine, respectively. Unfortunately, the placement of the two amino acids couldn't be revealed for serine and asparagine were the first shift of masses in the productions.

M3 (t_R = 1.984 min) with deprotonated molecular ion at *m/z* 471.1585, yielded corresponding fragment ions at *m/z* 297, 253, 251 and 120. The main product ion at *m/z* 297 $[M-H-71-103]^-$ was identical to the successive losses of alanine and cysteine. The fragment ion at *m/z* 253 was best explained by the cleavage of CO_2 (44 Da) from *m/z* 297 and its *othro*-allyl forming a five-membered ring by losing two hydrogen atoms caused the one at *m/z* 251. The further cleavage between the two benzene rings generated the ion at *m/z* 120. Based on the results discussed above, M3 was tentatively assigned as alanine and cysteine conjugation product, maybe the isomer of prevenient metabolites.

Metabolite M6 (t_R = 2.497 min) appeared $[M-H]^-$ at *m/z* 506.1119. Series of product ions at *m/z* 377, 344, 297, 281 and 263 were detected. The most meaningful

fragment ions at *m/z* 377[M-H-129]$^-$, 297[M-H129-80]$^-$ suggested M6 was a glutamic acid and sulfate conjugation product. The crucial fragment ion at *m/z* 344 derived from *m/z* 377 via losing hydroxyl and oxygen radical, which made the structure of M6 distinct. In regard to the ions at *m/z* 281 and 263 were produced by loss of oxygen atom from *m/z* 297(281 = 297-16) and further loss of a molecule of H_2O (263 = 281-18), respectively. As a result, it is reasonable to speculate the generation of M11 maybe as the following steps: the *para*-ally underwent hydroxylation and *othro*-allyl formed a five-memberd ring, then phenolic hydroxyl group and aliphatic hydroxyl group conjugated with sulfate and glutamic acid, respectively.

Conjugating with serine and sulfate generated metabolite M7 (t_R = 2.821 min) which was detected [M-H]$^-$ at *m/z* 464.1019 and generated fragment ions at *m/z* 377, 297, 265, 263. The dominating fragment ions at *m/z* 377 [M-H-87]$^-$ and 297 [M-H-87-80]$^-$ corresponded to the losses of serine and SO_3, respectively. The ion at *m/z* 297 losing two oxygen atoms induced the observation of deprotonated molecular ion of honokiol at *m/z* 265. The *ortho*-allyl of honokiol forming a six-memberd ring brought out the production at *m/z* 263.

M8 (t_R = 4.788 min), M14 (t_R = 14.056 min) and M16 (t_R = 15.183 min) yield deprotonated molecular ions at *m/z* 570.1930, 570.2240, 570.2239, respectively. The MS^2 spectrum of M8 showed fragment ions at *m/z* 306, 272, 254. The one at *m/z* 306 with high intensity was diagnostic deprotonated molecular ion of glutathione, which conjugated with honokiol to form the deprotonated molecular ion by losing two hydrogen atoms. Thus, M8 was tentatively identified as glutathione conjugation metabolite. The ions at *m/z* 272, 254 were products of glutathione, resulting from the elimination of H_2S (272 = 306-34) and further loss of H_2O (254 = 272-18), respectively.

As for M14 and M16, generated identical characteristic product ions at *m/z* 297, 254, 210. The common fragment ion at m/z 297 [M-H-$C_3H_5NO_2$-$C_{11}H_{10}N_2O$]$^-$ was formed by losses of serine and tryptophan from deprotonated molecular ion, indicating M14 and M16 were serien and tryptophan conjugates. The free radical fragment ion at *m/z* 254 originated from *m/z* 297 by the neutral loss of CO_2. Therefore,

the generation of M14 and M16 was tentatively deduced to be that *para*-allyl was oxidized to carboxyl, and the two phenolic hydroxyl groups of honokiol were position of serine and tryptophan conjugation.

M15 (t_R = 14.432 min) and M17 (t_R = 16.228 min) appeared $[M-H]^-$ at *m/z* 426.1554 and *m/z* 426.1551, respectively. The diagnostic fragment ions of M15 were at *m/z* 297, 256 (see Fig. 5(c)), while that of M17 was at *m/z* 297. The common fragment ion at *m/z* 297 $[M-H-129]^-$ indicated both them were glutamic acid conjugates. The loss of *ortho*-allyl free radical and the *para* aliphatic chain formed C=C bond, resulted in the fragment ion at *m/z* 256 of M15.

M18 (t_R = 19.118 min) and M19 (t_R = 21.298 min) gave the deprotonated molecular ions at *m/z* 384.1451 and 384.1445, respectively. The MS/MS spectra offered M18 fragment ions at *m/z* 297, 256 (see Fig. 5 (b)), while M19 generated product ions at *m/z* 297, 264, 263. Both them showed a primary fragment ion at *m/z* 297 $[M-H-87]^-$ which corresponded to the mass shift of serine (87 Da). The radical ion at *m/z* 256 of M18 could be attributed to cleavage of $-C_2H_3O$ from *m/z* 297 and the five-memberd ring opening by addition of two hydrogen atoms. The fragment ion at *m/z* 263 $[M-H-C_3H_5NO_2-H_2O-O]^-$ of M19 was subjected to *m/z* 297. Thus, M18 and M19 were elucidated to be serine conjugates, which also had been detected in rat fence [33]. Unfortunately, the site of serine was uncertain for the loss of serine happened first.

The deprotonated molecular ion of M20 (t_R = 21.956 min) was at *m/z* 441.1663, subsequent MS/MS analysis generated product ions at *m/z* 297, 264. The key product ion at *m/z* 297 $[M-H-C_2H_4NO-C_3H_7NO_2]^-$ unambiguously elucidated M20 was glycine and serine conjugation metabolite. Furthermore, by losses of hydroxyl group and oxygen free radical from *m/z* 297, producing the ion at *m/z* 264. Accordingly, the generation of M20 maybe that the two allyl groups of honokiol underwent hydroxylation, the two phenolic hydroxyl groups conjugated with glycine and serine subsequently.

3.2.3 Glucuronide metabolites (M4, M11-M13)

The mass shift of 176 Da and fragment ions at *m/z* 175, *m/z* 113 were representative characteristic of glucuronide conjugates, which were observed in the product ions of M4, M11, M12 and M13. Their possible structures were shown in Fig. 4.

In the MS spectrum under full scan mode, M4 (t_R = 2.189 min) showed the deprotonated molecular ion at *m/z* 537.1069, it gave the fragment ions at *m/z* 361, 281, 263, 175. Comparing with deprotonated molecular ion, diagnostic product ions at *m/z* 361 $[M\text{-}H\text{-}C_6H_8O_6]^-$ and *m/z* 281 $[M\text{-}H\text{-}C_6H_8O_6\text{-}SO_3]^-$ were in accord with correlative mass subtraction of 176 Da and 256 (176+80) Da. Hence, M4 was tentatively identified as glucuronide and sulfate conjugation product. Ion at *m/z* 263 resulted from that at *m/z* 281 by neutral loss of H_2O. The fragment ion at *m/z* 175 more plenary illustrated the validity of the above inference. By analyzing these fragmentation behaviors mentioned above, origin of M4 was tentatively concluded that the hydroxylation occurred on *ortho*-allyl with C=C double bond in a move, and then the two phenolic hydroxyl groups conjugated with glucuronic acid and sulfate.

M11 (t_R = 8.789 min) gave the deprotonated molecular ion $[M\text{-}H]^-$ at *m/z* 457.1497. The primary product ions were found at *m/z* 281, 240, 175, 113. On account of the product ion at *m/z* 281 $[M\text{-}H\text{-}176]^-$ was produced by the elimination of glucuronide, which consistent with the particular fragment ions of glucuronide at *m/z* 175, 113. As a result, M11 was identified as glucuronide conjugation product. The loss of C_2H_2OH from *m/z* 281 and the six-membered ring opening via addition of two hydrogen atoms, together contributed to the ion at *m/z* 240 with low intensity. Hence, *para*-allyl undergoing hydroxylation, the *ortho*-allyl forming a six-memberd ring, and then hydroxyl at C-2 position conjugating glucuronide, caused metabolite M11.

M12 (t_R = 10.670 min), M13 (t_R = 11.645 min) possessed the similar deprotonated molecular ions at *m/z* 441.1552, 441.1543, they were isomers of M20. In the MS/MS spectrum, common product ions at *m/z* 265, 224,113 were yield. The $[M\text{-}H]^-$ at *m/z* 441 was 176 Da more than that of honokiol. In addition, the ion at *m/z* 265$[M\text{-}H\text{-}176]^-$ further demonstrated that M12-M13 were glucuronide conjugates of honokiol. Honokiol contain two phenolic hydroxyl groups at C-2 and C-4' position,

which can form two glucuronide conjugates in theory.

3.4 Metabolic pathway of honokiol

By analyzing and comparing with previous reports, altogether 75 metabolites of honokiol in rat were detected and tentatively identified in our laboratory. It is obviously to found that: (1) both phase I metabolites and phase II metabolites could be observed in urine and feces, which focus on the excretion of honokiol; however only phase II metabolites were detected in plasma and small intestine, which highlights the distribution and metabolism; (2) the metabolites in plasma were mainly sulfate conjugates, while that in small intestine were mainly amino acid conjugates, also include several sulphated and glucuronide conjugates; (3) as summarized in Table 2, glucuronide conjugates could be detected in small intestine and plasma, while not been discovered in feces.

As a result, considering mentioned above and characteristics of metabolic *in vivo*, leading the deduction that honokiol enters the blood via intravenous, can rapidly transports through the bloodstream and immediately distributes into the intestinal lumen by secretion or diffusion from systemic circulation, or may be excreted in the bile, underwent hepatoenteral circulation could be reabsorbed as conjugates. Meanwhile, it is important not only to understand the roles of conjugation reaction in drug metabolism, but also to develop new drugs with high efficacy, quick metabolism, and small risk of side toxic effects, honokiol could be metabolized to conjugates with stronger polarity in small intestine which had the potential to facilitate their excretion. Moreover, amino acids conjugates, glucuronide conjugates and sulfate conjugates usually had no pharmacological activities and caused toxic effects seldom, which revealed that honokiol play the pharmacological activities by itself, rather than its metabolites.

4. Conclusions and prospective

In present study，detection and tentatively deduction of honokiol metabolites in rat small intestine were performed by UHPLC/Q-TOF-MS couple with ^{13}C stable isotopic labeling. It is the first report about metabolites in small intestine by this

method. As a result, altogether 20 metabolites were detected and identified, including 4 sulfate conjugates, 12 amino acids conjugates and 4 glucuronide metabolites, eight of which were first time to be reported. The results once again highlight the contribution of small intestine metabolism playing a significant role of drug metabolism. Furthermore, combining the results of this study with previous reports provided an integrative view on metabolic pathway of honokiol as a promising drug candidate with the potential clinical indication for the treatment of cancer, also reasonably promoted the study of honokiol on safety, toxicity, formulation development, ramification and so on.

Acknowledgements

This work was supported by the National Natural Science Foundation of China (81374017).

References

1 J. M. Lin, A. S. Prakasha Gowda, A. K. Sharma, and S. Amin, *Bioorg Med Chem.*, 2012, **20**, 3202-3211.

2 H. Kuribara , W. B. Stavinoha , and Y. Maruyama, *J. Pharm Pharmacol.*, 1998, **50**, 819-26.

3 P. Zhang, X. Y. Liu, Y. L. Zhu, S.Z. Chen, D. M. Zhou, and Y. Y. Wang, *Neurosci Lett.*, 2013, **534**, 123-127

4 J.J. Wang, R. Zhao, J. C. Liang, and Y. Chen, *Chinese Herbal Medicines*, 2014, **6**, 42-46.

5 L. Q. Qiang, C. P. Wang, F. M. Wang , Y. Pan, L. T. Yi , X. Zhang , and L. D. Kong , *Arch Pharm Res*, 2009 ,**32**, 1281-1292.

6 H. Hu, X. X. Zhang , Y. Y. Wang, and S. Z. Chen, Acta Pharmacol Sin, 2005, 26, 1063-1068.

7 H. Q. Yin, Y. C. Kim, Y. S. Chung, Y. C. Kim, Y. K. Shin, and B. H. Lee, *Toxicol Appl Pharmacol* 2009, **236**, 124–130.

8 Y. S. Kim, J. Y. Lee, J. Park, W. Hwang, J. Lee, and D. Park, *Arch Pharm Res*, 2010, **33**, 61-65.

9 Y. R. Lin, H. H. Chen, Y. C. Lin, C. H. Ko, and M. H. Chan, *J Biomed Sci.*, 2009, **16**, 94.

10 Z. Y. Hua, X. L. Bian, X. Y. Liu, Y. J. Zhu, X. Y. Zhang, S. Z. Chen, K. W. Wang, and Y. Y. Wang, *Brain Res.*, 2013, **1491**, 204–212.

11 P. Banerjee, A. Basu, J. L. Arbiser, and S. Pal, *Cancer Lett.*, 2013, **338**, 292-299.

12 Y. J Chen, C. L. Wu, J. F. Liu, Y. C. Fong, S. F. Hsu, T. M. Li, Y. C. Su, S. H. Liu, and C. H. Tang, *Cancer Lett.*, 2010, **291**, 20-30.

13 D. B. Avtanski, A. Nagalingama, M. Y. Bonner, J. L. Arbiser, N. K. Saxenad, and D. Sharma, *Mol Oncol.*, 2014, **8**, 565-580.

14 L. S Kaminsky, and Q. Y. Zhang, *Drug Metab Dispos.*, 2003, **31**, 1520-1525.

15 K. Thelen, and J. B. Dressman, *J Pharm Pharmacol.*, 2009, **61**, 541–558.

16 G. Iiizumi, Y. Sadoya, S. Hino, N. Shibuya, and H. Kawabata, *Biochim Biophys Acta.*, 2007, **1774**, 1289–1298.

17 M. Debiec-Rychter, S. J. Land, and C. M. King, *Cancer Lett.*, 1999, **143**, 99-102.

18 A. J. Molina, J. G. Prieto, G. Merino,G. Mendoza, R. Real, M. M. Pulido, and A. I. Alvaez, *Life Sci.*, 2007, **80**, 397-407.

19 D. Waziers I, P. H. Cugnenc, C. S. Yang, J. P. Leroux, and P. H. Beaune, *J Pharmacol Exp Ther.* 1990, **253**, 387–394.

20 G. M. Pacifici, M. Franchi, C. Bencini, F. Repetti, N. D. Lascio, and G. B. Muraro, *Xenobiotica* 1988, **18**, 849–856.

21 K. Engeland, and W. Maret, *Biochem Biophys Res Commun*, 1993, **193**, 47–53.

22 Q. Shan,Y.M. Liu, L. M. He, H. Z. Ding, X. H. Huang, F. Yang, and Y. F. Li, *J. Chromatogr. B Anal. Technol. Biomed. Life Sci.*, 2012, **881-882**, 96-106.

23 C. F. Luo, M. Yuan, M. S. Chen, S. M. Liu, and H. Ji, *J. Chromatogr. B Anal. Technol.Biomed. Life Sci.*, 2010, **878**, 363–370.

24 A. K. Sohlenius-Sternbeck, and A. Orzechowski, *Chem Biol Interact*, 2004, **148**, 49–56.

25 T. Sousa, R. Paterson, V. Moore, A. Carlsson, B. Abrahamssond, and A.W. Basit, *Int J Pharm.*, 2008, **363**, 1–25.

26 H. C Ren, G.J Wang, J. Y A, H.Y Xie, W. B Zha, B. Yan, F. Z Sun, H. P Hao, S.H Gu, L. S Sheng, F. Shao, J. Shi and F. Zhou, *J Pharm Biomed Anal.*, 2008, **48** 1476-1480.

27 E. Takach,T. O'Shea, and H. L. Liu, *J. Chromatogr. B Anal. Technol. Biomed. Life Sci.*, 2014, **doi**: 10.1016/j.jchromb.2014.04.043.

28 H. C. Liu, G. Ponniah, A. Neill, R. Patel, and B. Andrien, *J. Chromatogr. B Anal. Technol. Biomed. Life Sci.*, 2014, **958**, 90–95.

29 A. Stanislaus, K. Guo, and L. Li, *Anal Chim Acta.*, 2012, **750**, 161–172.

30 A. González-Antuña, J. C. Domínguez-Romero, J. F. García-Reyes, P. Rodríguez-Gonzáleza, G. Centineo, J. I . García Alonso, and A. Molina-Díaz, *J. Chromatogr. A.*, 2013, **1288**, 40–47.

31 J. Liu, M. H. Tang, H. J. Lai, Y. F. Dong, C. F. Xie, H. Y. Ye, L. Ma, N. Qiu, Y. F. Li, L. L. Cai, and L. J. Chen, *J. Chromatogr. A*, 2013, **1925**, 48-56.

32 H. J. Lai, M. H. Tang, J. Liu, Y. F. Dong, N. Qiu, S. C. Li, L. Ma, J. H. Yang, H. Song, Y. K. Zhang, A. H. Peng, and L. J. Chen, *J. Chromatogr. B Anal. Technol. Biomed. Life Sci.*, 2013, **931**, 157-163.

33 Y. F. Dong, M. H. Tang, H. Song, R. Li, C. Y. Wang, H. Y. Ye, N. Qiu, Y. K. Zhang, L. J. Chen, and Y. Q. Wei. *J. Chromatogr. B. Analyt. Technol. Biomed. Life Sci.*, 2014, **953–954**, 20–29.

34 A. H. Peng, H. Y. Ye, J. Shi, S. C. He, S. J. Zhong, S. C. Li, and L. J. Chen, *J. Chromatogr. A* 2010, **1217**, 5935.

35 M. Y. Liu, S. H. Zhao, Z. Q. Wang, Y. F. Wang, T. Liu, S. Li, C. C. Wang, H. T. Wang, and P. T. Tu, *J Chromatogr B Analyt Technol Biomed Life Sci.*, 2014, **949–950**, 115–126.

36 M. Hattori, T. Sakamoto, Y. Endo, N. Kakiuchi, K. Kobashi, T. Mizuno, and T. Namba, *Chem. Pharm. Bull.*, 1984, **32**, 5010.

37 B. Prasad, A. Garg, H. Takwani, and S. Singh, *Trend Anal. Chem.*, 2011, **30**, 360.40. H. C Ren, G.J Wang, J. Y A, H.Y Xie, W. B Zha, B. Yan, F. Z Sun, H. P Hao, S.H Gu, L. S Sheng, F. Shao, J. Shi and F. Zhou, *J Pharm Biomed Anal.*, 2008, **48**, 1476-1480.

Table 1

The UHPLC-MS data obtained in negative ion detection mode for honokiol mebabolites in rats small intestine after vien administration.

NO	Metabolic pathway (conjunction)	t_R (min)	Ion pair $[M-H]^-$ (Da)	Product ions$[M-H]^-$ (Da)	Formula	Error (ppm)
M1	Serine, Asp	1.522	482.1926-488.2233	281.1172, 263.1061,224.0842	$C_{25}H_{29}N_3O_7$	-0.41
M2	sulfation	1.813	349.0389-355.0603	269.0810, 225.0920, 209.0600, 184.0590, 183.0435	$C_{18}H_{22}O_5S$	1.43
M3	Ala, Cys	1.984	471.1585-477.1679	297.1120, 253.1240, 251.1080, 120.1697	$C_{24}H_{28}N_2O_6S$	1.06
M4	Glc	2.189	537.1069-543.1294	361.0743, 281.1187, 263.1065, 175.0342	$C_{24}H_{26}O_{12}S$	0.37
M5	sulfation	2.497	375.0541-381.0791	295.0976, 251.1068, 210.0688	$C_{18}H_{16}O_7S$	0.53
M6	sulfation, Glu	2.497	506.1118-512.1309	377.0692, 344.0720, 297.1129, 281.1173, 263.1081	$C_{23}H_{25}NO_{10}S$	-0.59
M7	sulfation, Ser	2.821	464.1019-470.1302	3770686, 297.1124, 265.232, 263.1077	$C_{21}H_{23}NO_9S$	0.65
M8	GSH	4.788	570.1930-576.1913	306.0758, 272.0872, 254.0769	$C_{28}H_{33}N_3O_8S$	3.51
M9	sulfation	7.592	361.0735-367.0914	281.1181, 240.1081	$C_{18}H_{18}O_6S$	-3.05
M10	sulfation	8.789	403.0851-409.1067	263.1076	$C_{20}H_{20}O_7S$	0.23
M11	Glc	8.789	457.1497-463.1723	281.1183, 240.1147, 175.0224, 113.0247	$C_{24}H_{26}O_9$	-0.44
M12	Glc	10.670	441.1552-447.1732	265.1224, 224.0846, 113.0252	$C_{24}H_{26}O_8$	0.45
M13	Glc	11.645	441.1543-447.1723	265.1239, 224.0843, 113.0246	$C_{24}H_{26}O_8$	-1.59
M14	GSH	4.788	570.1930-576.1913	306.0758, 272.0872, 254.0769	$C_{28}H_{33}N_3O_8S$	3.51
M15	Glu	14.432	426.1554-432.2008	297.1118, 256.0735	$C_{23}H_{25}NO_7$	0.23
M16	Ser, Try	15.183	570.2239-576.2493	297.1125, 254.1300,210.0675	$C_{32}H_{33}N_3O_7$	-0.35
M17	Glu	16.228	426.1551-432.1852	297.1129	$C_{23}H_{25}NO_7$	-0.47
M18	Ser	19.118	384.1451-390.1551	297.1114, 256.1095	$C_{21}H_{23}NO_6$	1.04
M19	Ser	21.289	384.1445-390.1704	297.1121, 264.1075, 263.1077	$C_{21}H_{23}NO_6$	-0.52
M20	Ser, Gly	21.956	441.1663-447.1844	297.1123, 264.1158	$C_{23}H_{26}N_2O_7$	0.23

Note: Ser=serine conjugation, Glu=glutamic conjugation, Gly=glycine conjugation, Ala=alanine conjugation, Cys=cysteine conjugation, Asp=asparagine conjugation, Try=tryptophan conjugation, Glc=glucuronic conjugation, GSH=glutathione conjugatio.

Table 2

Summary of honokiol phase II metabolites detected in rat fence, plasma and small intestine.

	$[M-H]^-$(Da)	Feces	Plasma	Small Intestine
Mono-sulfate conjugates	345.0795	√	√	ND
	345.0793	√	√	ND
	349.0389	ND	ND	√
	361.0744	√	√	ND
	361.0735	√	√	√
	375.0541	√	ND	√
	375.0542	√	ND	ND
	375.0899	ND	√	ND
	377.0694	√	√	ND
	377.0689	√	√	ND
	379.085	√	ND	ND
	379.0851	√	√	ND
	389.0698	ND	√	ND
	391.0848	√	√	ND
	401.0691	ND	√	ND
	403.0851	ND	ND	√
Amino acid conjugates	384.1445	√	ND	ND
	384.1449	√	ND	ND
	384.1451	√	ND	√
	384.1455	√	ND	√
	426.1554	√	√	√
	426.1551	√	√	√
	441.1663	ND	ND	√
	442.1499	√	ND	ND
	464.1019	√	ND	ND
	471.1585	ND	ND	√
	482.1926	ND	ND	√
	506.1118	ND	ND	√
	516.165	√	ND	ND
	516.1652	√	ND	ND
	570.193	ND	ND	√
	570.224	ND	ND	√
	570.2239	ND	ND	√
	596.1013	√	ND	ND
	682.2556	√	ND	ND
Glucuronide conjugates	441.1552	ND	√	√
	441.1543	ND	√	√
	457.1497	ND	√	√
	485.1445	ND	√	ND
	537.1069	ND	ND	√

√, detected; ND, not detected.

Figure Legends

Fig. 1 Chemical structures of honokiol and [^{13}C]-labeled-honokiol.

Fig. 2 The UPLC/Q-TOF-MS base peak chromatograms in negative ionization mode of experimental sample (A) and blank sample (B).

Fig. 3 The Q-TOF-MS spectra of six representative isotope clusters metabolites. (A) metabolite M5 (*m/z* 375.0541-381.0791); (B) metabolite M18 (*m/z* 384.1445-490.1704); (C) metabolite M7 (*m/z* 464.1019-470.1302); (D) metabolite M12 (*m/z* 441.1552-447.1732); (E) metabolite M11 (*m/z* 457.1497-463.1723); (F) metabolite M4 (*m/z* 537.1069-543.1294).

Fig. 4 Proposed structures of 20 honokiol metabolites in small intestine, new metabolites were underlined. (Ser=serine, Glu=glutamic, Gly=glycine, Ala=alanine, Cys=cysteine, Asp= asparagine, Try= tryptophan, Glc= glucuronic, GSH=glutathione).

Fig. 5 The representative MS/MS spectra of four metabolites. (A) metabolite M9 (*m/z* 361); (B) metabolite M18 (*m/z* 384); (C)metabolite M15 (*m/z* 426) ; (D) metabolite M13 (*m/z* 441).

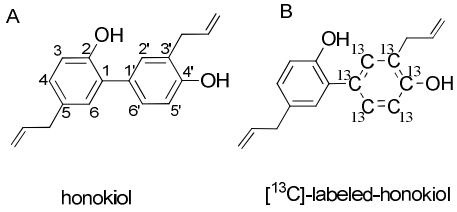

Fig. 1 Chemical structures of honokiol and [^{13}C]-labeled-honokiol.

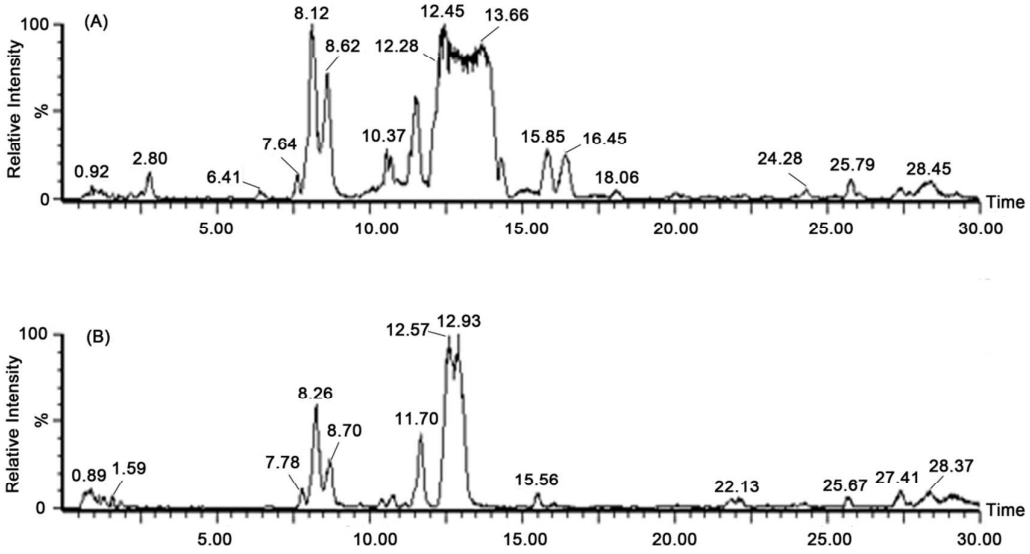

Fig. 2 The UPLC/Q-TOF-MS base peak chromatograms in negative ionization mode of experimental sample (A) and blank sample (B).

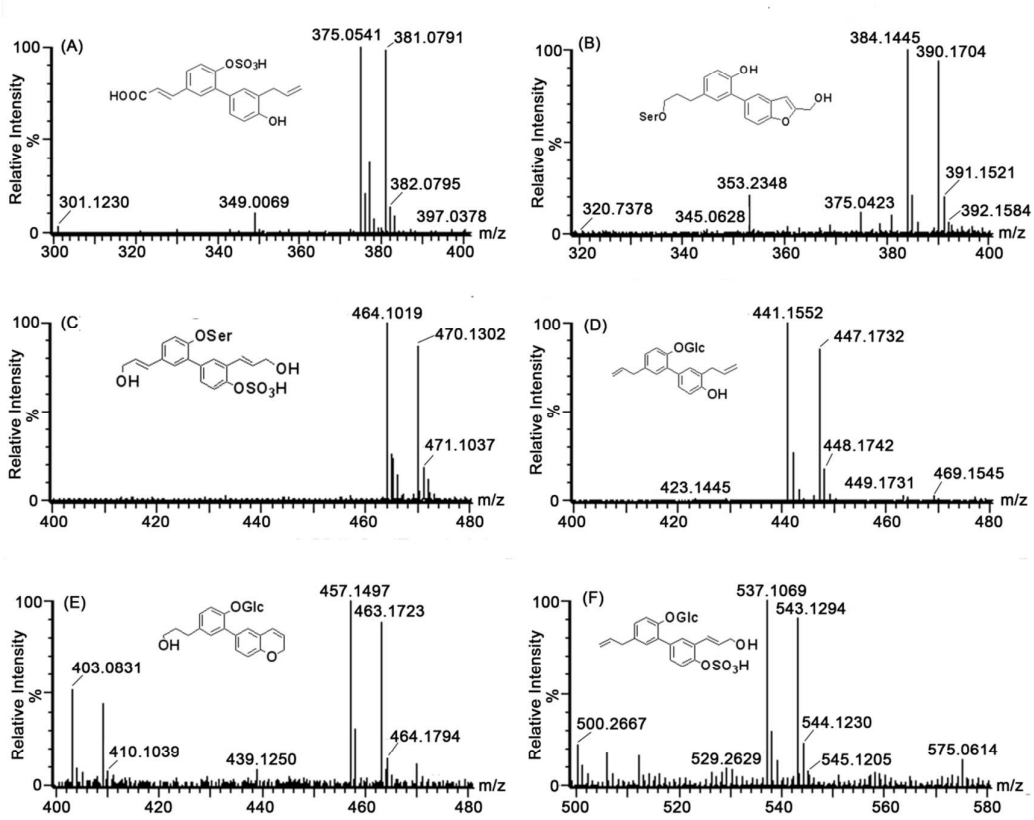

Fig. 3 The Q-TOF-MS spectra of six representative isotope clusters metabolites. (A) metabolite M5 (*m/z* 375.0541-381.0791); (B) metabolite M18 (*m/z* 384.1445-490.1704); (C) metabolite M7 (*m/z* 464.1019-470.1302); (D) metabolite M12 (*m/z* 441.1552-447.1732); (E) metabolite M11 (*m/z* 457.1497-463.1723); (F) metabolite M4 (*m/z* 537.1069-543.1294).

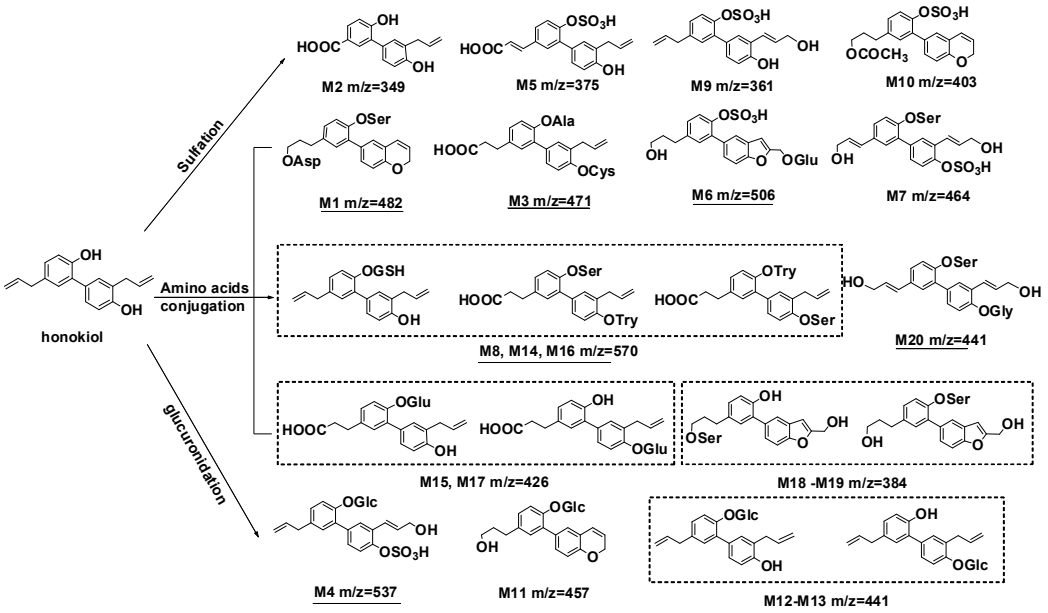

Fig. 4 Proposed structures of 20 honokiol metabolites in small intestine, new metabolites were underlined. (Ser=serine, Glu=glutamic, Gly=glycine, Ala=alanine, Cys=cysteine, Asp= asparagine, Try= tryptophan, Glc= glucuronic, GSH=glutathione)

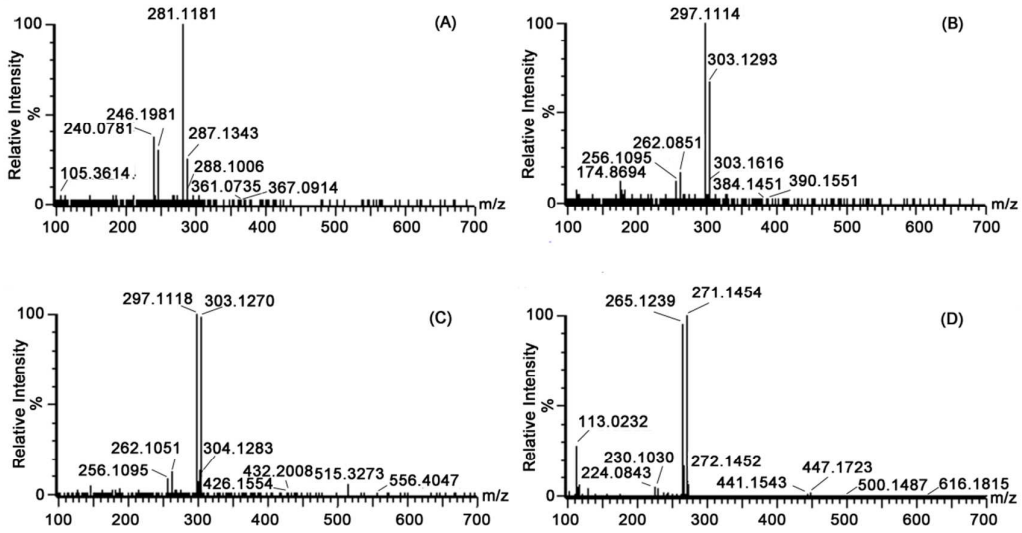

Fig. 5 The representative MS/MS spectra of four metabolites. (A) metabolite M9 (*m/z* 361); (B) metabolite M18 (*m/z* 384); (C)metabolite M15 (*m/z* 426) ; (D) metabolite M13 (*m/z* 441)